symmetry

IMPACT FACTOR 2.2

CITESCORE 5.4

Article

Evaporation of Primordial Charged Black Holes: Timescale and Evolution of Thermodynamic Parameters

José Antonio de Freitas Pacheco

Special Issue
Symmetry in Gravity Theories and Cosmology

Edited by
Dr. Sunil Kumar Tripathy, Dr. Dipanjali Behera and Dr. Hooman Moradpour

MDPI

https://doi.org/10.3390/sym16070895

symmetry

MDPI

Article

Evaporation of Primordial Charged Black Holes: Timescale and Evolution of Thermodynamic Parameters

José Antonio de Freitas Pacheco

Université de la Côte d'Azur—Observatoire de la Côte d'Azur, 06304 Nice, France; pacheco@oca.eu

Abstract: The evolution of primordial black holes formed during the reheating phase is revisited. For reheating temperatures in the range of 10^{12}–10^{13} GeV, the initial masses are respectively of the order of 10^{10}–10^{8} M_P, where M_P is the Planck mass. These newborn black holes have a small charge-to-mass ratio of the order of 10^{-3}, a consequence of statistical fluctuations present in the plasma constituting the collapsing matter. Charged black holes can be rapidly discharged by the Schwinger mechanism, but one expects that, for very light black holes satisfying the condition $M/M_P << M_P/m_W$ (m_W is the mass of the heaviest standard model charged W-boson), the pair production process is probably strongly quenched. Under these conditions, these black holes evaporate until attaining extremality with final masses of about 10^{7}–10^{5} M_P. Timescales to reach extremality as a function of the initial charge excess were computed, as well as the evolution of the horizon temperature and the charge-to-mass ratio. The behavior of the horizon temperature can be understood in terms of the well-known discontinuity present in the heat capacity for a critical charge-to-mass ratio $Q/\sqrt{G}M = \sqrt{3}/2$.

Keywords: charged black holes; luminosity evolution; dark matter

Citation: de Freitas Pacheco, J.A. Evaporation of Primordial Charged Black Holes: Timescale and Evolution of Thermodynamic Parameters. *Symmetry* **2024**, *16*, 895. https://doi.org/10.3390/sym16070895

Academic Editors: Sunil Kumar Tripathy, Dipanjali Behera, Hooman Moradpour and Kazuharu Bamba

Received: 19 April 2024
Revised: 21 June 2024
Accepted: 25 June 2024
Published: 13 July 2024

1. Introduction

The non-detection of supersymmetric signals in experiments performed with the Large Hadron Collider led to the abandonment of the idea that particles issued from minimal extension theories of the Standard Model could be the major constituents of dark matter [1]. Consequently, old suggestions proposing that dark matter particles could be primordial black holes [2,3] have been revived in the past years. Black holes with masses less than the solar value that could be formed early in the universe were analyzed by [2], while [3] postulated that as a consequence of the Hawking evaporation process, black hole relics with Planck masses (M_P) result and could constitute the dark matter present in the universe. Notice that, postulating the existence of stable Planck mass relics, quantum effects were indirectly considered since this is equivalent to saying that the black hole horizon radius cannot be smaller than the Compton wavelength associated with the black hole itself.

In a flat Friedmann–Robertson–Walker universe, primordial black holes (PBHs) with masses in the range of 10^{6}–10^{9} M_P are expected to be formed at the end of the inflation, during the oscillatory and decay phase of the inflaton field or during the reheating [4–10]. They may also be formed naturally at high peaks of the curvature power spectrum resulting from a single-field inflation [11]. According to the scenario developed by [12], PBHs can be formed at the end of the inflationary era during a long oscillatory phase of the inflaton field that extends the reheating timescale. In this picture, PBHs have a characteristic mass $M \simeq 4\pi(M_P^2/H_*)$, where H_* is the Hubble scale during inflation. In the slow-roll approximation, we have $H_* \simeq (\pi/16)M_P^2 r A_s$, where r is the amplitude ratio between the tensor and the scalar power spectra and A_s is the amplitude of the scalar power spectrum. Using data from Planck-2018, one obtains $H_* \simeq 10^{13}$ GeV, which implies a typical mass of about $10^6 M_P$ for primordial black holes formed in this scenario.

Two main aspects play a central role in the formation process: first, for each horizon-sized space-time region, there exists a critical threshold value for the density (or mass)

contrast δ_c that separates the late evolution between the formation of a black hole and the dispersion of the perturbation by pressure forces; second, when the overdensity perturbation is close to the critical value, the final mass of the black hole may be a small fraction of the horizon mass [13]. However, as we shall see later, the Bekenstein entropy bound [14] fixes a minimum mass that is able to collapse and form a black hole.

One of the great difficulties with these light PBHs is their short lifetime against the Hawking evaporation mechanism, since only PBHs with masses greater than 3×10^{14} g can survive up to today. The evaporation process can be quenched if black holes are extremal since, in this case, the horizon temperature is zero, extinguishing the emission process. Extremal black hole solutions can be obtained in Kerr (K) or in Reissner–Nordstrom (RN) space-times as well as in some non-singular metrics [15]. In the case of rotating black holes, it has been argued [16] that, besides mass, angular momentum is also lost during the evaporation process, and consequently, an extremal condition is difficult to be maintained under these circumstances. This difficulty can be circumvented if Planck-sized BHs are quantized [17], since, in this case, a stable fundamental state exists with a mass equal to the Planck value and spin $J = \hbar$. Another alternative was discussed by [18], who considered asymptotically free gravitational theories with a limiting curvature in which stable remnant solutions exist. The horizon temperature in these relics is zero, and their masses are determined by the inverse limiting curvature.

A charged (RN) black hole is also an alternative permitting extremal solutions. However, there are two major obstacles for the existence of charged BHs in nature. The first is the Schwinger mechanism, which is able to neutralize the BH charge in a very short timescale [19,20]. In other words, the presence of an intense electric field across the BH horizon changes the vacuum polarization state and separates virtual particle–anti-particle pairs [21]. Particles with the same BH charge are "repelled", while particles with an opposite charge cross the horizon, contributing to discharging the BH. However, the usual equations describing the Schwinger pair production rate near the BH horizon are valid only if the horizon radius of the black hole is larger than the Compton wavelength of the related particle [22,23], or in other words, the condition $(M/M_P) > (M_P/m)$ must be satisfied (however, see an opposite argument in [20]). Boson and fermion pairs can be produced by the Schwinger mechanism, and when the aforementioned condition is applied to the heaviest charged bosons $W^{\pm}$, the black hole mass should satisfy $M > 4.1 \times 10^{12}$ g in order that the discharge process would be efficient. As we shall see, PBHs considered in the present investigation have masses much smaller than this limit, and consequently, we could expect that the neutralization of the BH charge by this mechanism would be strongly weakened. Unfortunately, for "light" BHs, no explicit relation for the pair production rate is available in the literature, but some numerical calculations by [24] point to the following reduction factors: for a ratio between the horizon radius and the Compton wavelength $GMm/\hbar c = 0.271$, the production rate is decreased by 10%, while for a ratio $GMm/\hbar c = 0.160$, the production rate is reduced by one-half. This picture is not substantially modified if, besides the charge, the BH has some angular momentum [25]. It is worth mentioning that the Hawking emission mechanism, although at a slower rate, may also contribute to neutralizing the black hole. If $\pm e$ is the charge of the emitted particle and ϕ_H is the electric potential at the BH horizon, the electrostatic energy term $\pm e\phi_H$ contributes to the chemical potential of the particle, introducing a slight asymmetry in the emission process. Particles having charges with the same signal as that of the BH are emitted preferentially and hence contribute to the neutralization of the BH [20].

As we shall see below, dynamical studies suggest that the newborn BH is not in an extremal state, and in such a situation, the BH loses mass due to the Hawking mechanism, approaching an extremal condition if the Schwinger process is in fact quenched as one expects for light black holes. In the present investigation, primordial black holes formed at the reheating epoch are considered. These black holes are expected to have a small electric charge, a consequence of Poisson fluctuations present in the collapsing volume. If this is the case, once formed, the black hole begins to evaporate, increasing its charge-to-mass ratio

until the extremal condition is fulfilled. In this state, the black hole is stable and could be a possible candidate to explain the nature of dark matter particles. In this paper are reported new numerical calculations of the evaporation lifetime of an initially charged black hole, and a comparison is performed with the well-known results for Schwarzschild BHs. The time evolution of the luminosity and of the horizon temperature are also computed, both having a behavior distinct from those of a non-charged BH. In particular, when the initial charge-to-mass ratio satisfies the condition $Q/\sqrt{G}M \geq \sqrt{3}/2$, the horizon temperature decreases as the evaporation proceeds, since the heat capacity becomes positive beyond the aforementioned critical value of the charge-to-mass ratio. The paper is organized as follows: in Section 2, the black hole formation scenario is discussed and the initial charge-to-mass ratio is estimated; in Section 3, numerical examples are presented, as well as "classical" calculations of the evaporation lifetime of a charged BH, keeping constant its initial charge; and in Section 4, the main conclusions are given.

2. The BH Formation Scenario

Presently, there is no consensus among in scientific community concerning the mechanisms able to produce a charge separation during the gravitational collapse. Some possible scenarios have been reviewed in [26], including, in particular, the possibility that an initial charge excess produced by statistical fluctuations could be present in the collapsing matter. However, the resulting initial charge-to-mass ratio due to such a mechanism is expected to be small and, hence, unable to avoid the loss of a substantial fraction of the initial mass by the Hawking evaporation process. In fact, some dynamical studies indicate the formation of a non-extremal black hole as a consequence of the gravitational collapse of electrically charged matter [27]. Late evolutionary phases are dominated by the Hawking evaporation as the BH approaches extremality. The presence of a charge excess during the collapse of massive perturbations may produce some unexpected effects as, for instance, the Cauchy horizon may be replaced by a space-like central singularity that depends on the value of the critical Schwinger field [28].

The maximum expected mass M_H collapsing into a BH corresponds to scales comparable to the Hubble radius [29]. Past numerical studies of the gravitational collapse considered different setups [30–32], concluding that scaling and self-similarity solutions exist near the threshold of black hole formation. In general, the resulting black hole mass scales as $M \propto K(\delta - \delta_c)^\gamma$, where $\delta_c \simeq 0.45$ is the critical density contrast above which black hole formation occurs, and $K \simeq 3.3$ and $\gamma \simeq 0.36$ are constants whose values have been empirically determined [13,32,33]. More recently, a new investigation on the density contrast threshold for black hole formation confirms those values derived by numerical experiments [34]. Here, we adopt such results, and consequently, the mass of the newborn BH can be expressed as

$$M = K(\delta - \delta_c)^\gamma M_H \tag{1}$$

Assuming that BHs are formed during or just after reheating, the mass inside the Hubble radius is given by

$$\frac{M_H}{M_P} = \sqrt{\frac{45}{16\pi^3}}\, g_{ef}^{-1/2} \left(\frac{M_P}{T_{rh}}\right)^2 \tag{2}$$

In the above equation g_{ef} is the effective number of degrees of freedom of the cosmic plasma constituted by SM particles. Notice that, in principle, very small black holes could be formed considering density fluctuations close to the critical value δ_c. However, there is a lower limit for the BH mass imposed by the Bekenstein "universal" entropy bound [14]. In other words, the entropy of the collapsing matter must be smaller than that of the resulting black hole. This condition imposes a lower bound for the BH mass given by

$$\frac{M}{M_P} \geq \frac{1}{3\pi\beta}\left(\frac{M_P}{T_{rh}}\right)(1+\varepsilon)^{-2} \tag{3}$$

In Equation (3), the parameter β represents the efficiency of the gravitational collapse, taking into account, for instance, radiative losses. The charge-to-mass ratio parameter ε was defined as in [35], i.e.,

$$\varepsilon^2 = 1 - \frac{Q^2}{GM^2} \tag{4}$$

where Q is the BH charge. Notice that an extremal RN black hole occurs when $\varepsilon \to 0$, and when $\varepsilon \to 1$, the usual Schwarzschild case is recovered. With this definition of the charge-to-mass parameter, the horizon radius of an RN black hole can be written as $r_H = (GM/c^2)(1+\varepsilon)$. Combining Equations (2) and (3) implies that

$$(\delta - \delta_c)^\gamma \geq \frac{1.41}{(1+\varepsilon)^2}\left(\frac{M_P}{T_{rh}}\right)^{-1} \tag{5}$$

and the numerical factor was obtained by assuming $\beta = 0.8$. For example, for $T_{rh} = 10^{13}$ GeV and $\varepsilon = 0.1$, the Bekenstein bound is satisfied if $\mid \delta - \delta_c \mid > 2 \times 10^{-17}$.

In order to perform numerical calculations, the initial mass M_0 of the BH was estimated under the assumption that mass density fluctuations have a Gaussian distribution. In this case, defining $x = \mid \delta - \delta_c \mid$, the BH number density distribution is given by

$$\frac{dN_{BH}}{dM} = \frac{dN_{BH}}{d\delta}\frac{d\delta}{dM} \propto x^{1-\gamma} e^{-\frac{(x+\delta_c)^2}{2\sigma_0^2}} \tag{6}$$

and shown in Figure 1. For the mean square density fluctuation, we adopted the value $\sigma_0 \simeq 6.0 \times 10^{-5}$ that results from the observed temperature fluctuation present in the the cosmic microwave background angular power spectrum, assuming an adiabatic relation between these two thermodynamic variables. In this case, the distribution in Figure 1 peaks approximately at $\mid \delta - \delta_c \mid = 5.12 \times 10^{-9}$, corresponding to a BH mass of $M = 3.42 \times 10^{-3} M_H$, a value adopted as the representative mass of primordial black holes in our scenario. In order to compute the mass inside the horizon, two values for the reheating temperature were assumed, respectively, equal to 10^{12} GeV and 10^{13} GeV. These values are consistent with an upper limit of 10^{14} GeV obtained by [36] and with estimates by [37] derived from different inflaton decay models. In this case, the horizon masses corresponding to the assumed reheating temperatures are, respectively, $4.33 \times 10^{12}\ M_P$ and $4.33 \times 10^{10}\ M_P$, and the resulting initial BH masses are, respectively, $M \simeq 1.48 \times 10^{10}\ M_P$ and $M \simeq 1.48 \times 10^{8}\ M_P$. A similar analysis was performed in [33], but the authors considered Gaussian fluctuations without the presence of a critical density and late formation epochs. Consequently, they have obtained more massive black holes. It is worth mentioning that, due to the Bekenstein limit, the minimum BH masses are about $10^7\ M_P$ and $10^5\ M_P$, respectively, for $T_{rh} = 10^{12}$ GeV and 10^{13} GeV.

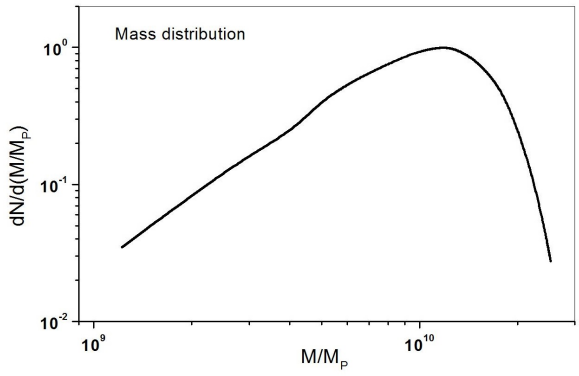

Figure 1. Number density of black holes formed per unit of mass as a function of the black hole mass in units of the Planck mass. The vertical axis has relative units due to the normalization procedure adopted to perform the plot.

The Initial Charge-to-Mass Ratio

In the present scenario, we assume that a slight charge excess due to Poisson fluctuations is initially present in the collapsing matter. Requiring that the total number of both positive (N_+) and negative (N_-) charges obeys the Poisson statistics, define the variable Δ such as $\Delta = (N_+ - N_-)$, which obeys the Skellam distribution. Clearly, the average value of such a variable is $< \Delta >= 0$, while the variance is $< \Delta^2 >= 2N$, with N standing for the mean value of either positive or negative charges. With these definitions, the expected initial charge excess Q within the collapsing volume is given by the variance of the Skellam distribution, or in other words,

$$Q^2 = 2\alpha\delta_+^2(\hbar c)N \tag{7}$$

where α is the electromagnetic fine structure constant and $\delta_+ = 0.597$ is the mean SM charge per particle once heavy charged bosons, leptons, and quarks are present in the cosmic plasma at reheating. The total number of charged particles (positive or negative) is given by $n_{ch}V_c$, where n_{ch} is the charge density and V_c is the collapsing volume that can be written as $V_c = Mc^2/\rho$, where M is the black hole mass and ρ is the energy density of the cosmic plasma at reheating. Using the usual relativistic expressions for the energy and particle density, one obtains, after some algebraic manipulation,

$$\frac{Q^2}{GM^2} = 60\,\alpha\delta_+^2\left(\frac{g^+}{g_{ef}}\right)\frac{\zeta(3)}{\pi^4}\left(\frac{M_P}{M}\right)\left(\frac{M_P}{T_{rh}}\right) \tag{8}$$

where g^+ and g_{ef} are, respectively, the numbers of degrees of freedom appearing in the number charge density and in the energy density. Replacing Equations (1) and (2) into Equation (8), one obtains

$$\frac{Q^2}{GM^2} = \frac{80}{\sqrt{5\pi^5}}\frac{g^+\zeta(3)}{g_{ef}^{1/2}}\frac{\alpha\delta_+^2}{(K\mid\delta-\delta_c\mid^\gamma)}\left(\frac{T_{rh}}{M_P}\right) \tag{9}$$

Numerically, we have

$$\frac{Q}{\sqrt{G}M} = 2.46\sqrt{\frac{T_{rh}}{M_P}} \tag{10}$$

For the aforementioned reheating temperatures, i.e., 10^{12}–10^{13} GeV, one obtains, respectively, charge-to-mass ratios $Q/\sqrt{G}M = 7.04\times10^{-4}$ and 2.22×10^{-3}. Hence, as expected, the statistical charge fluctuation mechanism is not efficient enough to produce extremal black holes, and in fact, these objects have very small charge-to-mass ratios, implying an important mass loss by the Hawking evaporation mechanism before reaching extremality.

3. Hawking Evaporation of a Charged Black Hole

As seen above, black holes formed at the reheating phase may have a charge (positive or negative) acquired as a consequence of statistical fluctuations within the collapsing region. Since the initial charge-to-mass ratio is quite small, these black holes begin to evaporate. We expect that, while they lose mass during the evaporation process, their charge is kept more or less constant since the Schwinger mechanism is probably quenched by the fact that the horizon radius of these black holes is much smaller that the Compton wavelength of the heaviest standard model charged boson. It is worth mentioning that once extremality is reached, such an argument is reinforced since the horizon radius has considerably shrunk. Moreover, the charge stability in a quasi-extremal situation was also investigated by [38], who proposed a thermal interpretation of the Schwinger effect. The authors assumed that the Schwinger temperature is equivalent to the Davies–Unruh temperature of particles accelerated by the electric field of the black hole and the scalar curvature of an $AdS_2 \times S_2$ geometry. As a consequence, they found a charge upper bound for an extremal black hole to remain stable against the Schwinger effect. The evaporation

of a charged black hole, including also the discharge by the Schwinger mechanism, was investigated by [39], but only massive black holes were considered since, for these objects, no restrictions exist concerning the quenching condition discussed above.

In these conditions, it is interesting to estimate the timescale required to reach extremality since the initial charge-to-mass ratio considerably affects the evaporation rate. The evaporation process of quasi-extremal black holes was considered, among others, in [40], which adopted the Vaidya metric; that is, the mass parameter varies, but the charge is kept constant. Here, similar computations were performed in order to estimate the timescale necessary to attain extremality. Small charge variations due to the slight asymmetry in the emission of charged particles were neglected since the BH was assumed to radiate like a "grey" body. The "grey" body factor Γ_s is related to the absorption cross section σ_s by the relation

$$\Gamma_s = \frac{\sigma_s}{\pi}\left(\frac{E}{\hbar c}\right)^2 \tag{11}$$

where s and E are, respectively, the spin and the energy of the particle. Recent calculations of grey body factors can be found in [41,42]. Including corrections due to the presence of a charge in the expression of the horizon area and temperature, the mass loss rate can be expressed by the equation

$$\frac{dM}{dt} = -\beta\left[\frac{\hbar c^4}{(GM)^2}\right] f(\varepsilon) \tag{12}$$

where $f(\varepsilon) = \varepsilon^4/(1+\varepsilon)^6$ and the parameter ε was already defined by Equation (4). The parameter β depends on the grey body factors and, hence, on the black hole mass, including the contribution of all fields emitted in the temperature (mass) range of interest. Notice that for light BHs, as those considered here, the Hawking radiation is constituted essentially by photons, neutrinos, and gravitons. For Schwarzschild black holes, numerical values of β were obtained in [43] and, more recently, in [42]. Here, we have estimated $\beta = 2.34 \times 10^{-2}$, a value that agrees with the results in [43] when $\varepsilon \to 1$, a limit corresponding to Schwarzschild black holes of a small mass (or high horizon temperature). It is worth mentioning that, in the context of effective gravity field theories, second (and even third)-order terms have been introduced in the Schwarzschild metric, aiming to represent quantum corrections [44,45]. These terms are responsible for the appearance of a Cauchy horizon and higher-order corrections to the (area) entropy. The horizon temperature is also affected by these quantum effects, but corrections are important only for black holes having a few Planck masses [46] and, hence, not relevant to the primordial black holes considered here.

Equation (12) can be written in a dimensionless form by defining the new variables $y = M/M_0$, where M_0 is the initial black hole mass and $\tau = t/t_*$, where t_* is a characteristic timescale defined below. In this case, the equation above can be recast as

$$\frac{dy}{d\tau} = -\frac{f(y)}{y^2} \tag{13}$$

with the characteristic timescale t_* being defined by

$$t_* = \frac{t_P}{\beta}\left(\frac{M_0}{M_P}\right)^3 \tag{14}$$

where t_P is the Planck time. Using Equation (4), the function $f(y)$ can be explicitly written as

$$f(y) = \left(1 - \frac{y_f^2}{y^2}\right)^2 \left[1 + \sqrt{1 - \frac{y_f^2}{y^2}}\right]^{-6} \tag{15}$$

where the ratio between the final and initial BH masses $y_f = M_f/M_0$ was introduced. It should be emphasized that the parameter y_f depends only on the initial charge-to-mass ratio, that is, $y_f = Q/\sqrt{G}M_0$. Notice that the differential Equation (13) takes into account the variation of the particle emission rate not only because the BH mass decreases but also because the charge-to-mass ratio ε changes as the BH loses mass. Equation (13) should be solved with the initial condition $y(0) = 1$. Then, the dimensionless evaporation timescale τ_* is obtained when the extremal condition is reached, i.e., when $y(\tau_*) = y_f$, which is equivalent to the condition $\varepsilon(\tau_*) = 0$. The dependence of evaporation lifetime (t_{ev}) on the initial BH mass appears explicitly in the definition of the scale factor t_* (Equation (14)) since $t_{ev} = t_*\tau_*$. It should be emphasized that t_{ev} is, in fact, the timescale for the BH to reach extremality since a remnant is left.

It is important to say few words about some conceptual aspects concerning the evaporation timescale. The solution of the evaporation equations assumes an asymptotically flat space-time, but strictly speaking, black holes are imbedded in an expanding cosmological background. This problem was already discussed 80 years ago by Einstein and Strauss [47], who investigated the boundary conditions between a static Schwarzschild metric and an expanding background modeled as fluid having an uniform density and zero pressure. Lately, these junction conditions (known today as Israel conditions [48]) were also discussed, among others, in [49–52]. In general, the inner Schwarzschild space-time is expressed in terms of curvature coordinates (R, T), while beyond the boundary, the cosmological metric is expressed in terms of coordinates (R, τ), where τ is the time measured by geodesic clocks fixed in the cosmological fluid, which serves as a source in Einstein's equation. The transformation between the time coordinate T and the geodesic time τ can be found, for instance, in [50,53]. Hence, for a distant comoving observer located in the cosmological background, the measured Hawking energy flux is not exactly the same as that expected for a distant observer from the black hole. According to [53], Equation (13) should be corrected by a function $f(\epsilon)$ that decreases the mass loss rate. The variable ϵ is essentially given by the ratio between the black hole horizon radius and the Hubble radius, that is, $\epsilon = 2GMH/c^3$. Considering only first-order terms, the correction factor is given by [53]

$$f(\epsilon) \simeq (1 - 2\epsilon^{1/3}) \tag{16}$$

Such a correction is more relevant just after the black hole formation since once the evaporation begins, the event horizon shrinks and the Hubble radius grows as the universe expands, decreasing the value of ϵ. For the black hole masses considered in the present work, one has $\epsilon^{1/3} \simeq 9 \times 10^{-5}$, indicating that the difference in the mass loss rate measured between distant observers using curvature time or geodesic time is very small.

Just after formation, these PBHs begins to evaporate, but they can also accrete mass. Accretion may counterbalance losses by evaporation or affect the stability when extremality is attained. The accretion rate of relativistic matter was computed in [54] and is given by

$$\frac{dM}{dt} = g(\varepsilon)\pi\frac{(GM)^2}{c^5}\rho(T) \tag{17}$$

where $\rho(T)$ is the energy density of the cosmic plasma and the function $g(\varepsilon)$ depends on the charge-to-mass-ratio. For small values of the charge-to-mass ratio, $g(\varepsilon) \simeq 55.42$, while for an extremal black hole, $g(\varepsilon) \simeq 32.84$. Thus, the accretion efficiency decreases for an increasing charge. The accretion timescale is of the order of $\mid M/(dM/dt) \mid$, and for a temperatures of about $T \sim 10^{12}$ GeV, it is of the order of 10^{-19} s. This timescale is quite short but longer than the evaporation timescale, and one should expect that the evolution of the black hole mass is not too much affected by such a process [55]. Moreover, the energy density of the relativistic matter depends on the fourth power of the temperature, and due to the expansion of the universe, the temperature decreases rapidly over a timescale $\mid T/(dT/dt) \mid = H^{-1}$, which is of the order of 10^{-30} s, still shorter than the accretion time-scale. Hence, the adiabatic cooling of the universe inhibits the growth of the black

hole, which will not be affected by the accretion process. In fact, we have included an accretion term on the right side of Equation (13), and our results without such a term are not modified.

Numerical solutions of Equation (13) for different values of the initial charge-to-mass ratio permit for obtaining how the Hawking evaporation lifetime is affected by the presence of a charge. Numerically, we have assumed that extremality is attained when the condition $\varepsilon(\tau_*) \leq 10^{-15}$ is satisfied. However, for values of $y_f \geq 0.02$, the latter condition is approached very slowly and another time variable x was introduced in Equation (13) by defining $x = lg(1+\tau)$. With this definition, the initial condition is not modified since $\tau = 0$ implies also that $x = 0$ and Equation (13) becomes

$$\frac{dy}{dx} = -e^x \frac{f(y)}{y^2} \tag{18}$$

Results of these calculations are shown in Figure 2. Inspection of Figure 2 indicates that the evaporation lifetime increases noticeably only for initial charge-to-mass ratios higher than ∼0.02, as already mentioned, and tends toward "infinity" as $y_f \to 1$. In our scenario, the initial charge-to-mass ratio acquired by statistical Poisson fluctuations is quite small, and hence, the lifetime to reach extremality does not differ considerably from the value of the (total) evaporation lifetime of a Schwarzschild black hole having the same mass.

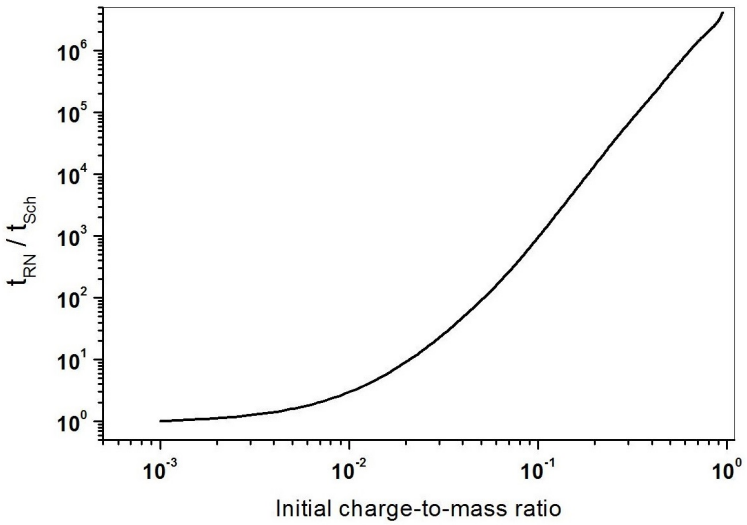

Figure 2. Ratio between the evaporation lifetime of a Reissner-Nordstrom and that of a Schwarzschild black hole as a function of the initial charge-to-mass ratio.

The evolution of a charged BH during the evaporation process differs in some distinct aspects from that describing a Schwarzschild BH. First, it is necessary to recall that the energy of a Schwarzschild black hole differs from that of an RN black hole. The energy of the former is simply associated with its mass, that is, $E = Mc^2$, while the energy of the latter also depends on the electric field potential. In the general relativity theory, the equivalence between mass and energy means that only combined effects can be measured by distance observers. In other words, the mass/energy contained in an arbitrary space-time volume is not well-defined and the energy–momentum tensor of matter plus all non-gravitational fields no longer satisfies the condition $T^k_{k;i} = 0$. Hence, the contribution from the gravitational field (or that of any other field) must be included in the construction of an adequate energy–momentum quantity that satisfies the divergence relation like the one in a flat space-time. Despite the many attempts to solve this problem in the past decades [56–58], there is still no agreed definition, except at infinity in asymptotically flat space-times. In fact, the energy–momentum of the gravitational field is a pseudo-tensor that explicitly depends

on the metric, and its first derivative vanishes in a locally flat space-time due to the strong equivalence principle.

Due to the absence of a local energy density of the gravitational field, it is tempting to introduce a meaningful quasi-local energy defined inside a given bounded region of the space-time. In fact, some useful definitions of such a quasi-local energy exist in the literature as, for instance, the Brown–York energy [59], the Hawking–Hayward energy [60,61], the Chen–Nester energy [62], and the Misner–Sharp (MS) energy [63]. Since the MS energy is defined in a spherically symmetric space-time, we will adopt such a formulation to estimate the energy (or effective mass) of a Reissner–Nordstrom black hole. It should be mentioned that the relation derived from the MS approach agrees with that resulting from the gravitational pseudo-tensor defined by Einstein [57]. Since the metric of an RN black hole is spherically symmetric, it can be represented as

$$ds^2 = h_{ab}dx^a dx^b + r^2 d\Omega_2^2 \tag{19}$$

where $d\Omega_2^2 = \sin^2\theta d\theta d\phi$ and the indices a, b correspond, respectively, to the coordinates t, r. The two-tensor h_{ab} can be represented by the matrix

$$h \equiv \begin{pmatrix} -f(r) & 0 \\ 0 & 1/f(r) \end{pmatrix} \tag{20}$$

Under these conditions, the MS energy inside a volume of ab areal radius r is (geometric units used)

$$E_{MS} = \frac{r}{2}\left(1 - h^{ab}\partial_a r \partial_b r\right) \tag{21}$$

For an RN black hole

$$f(r) = 1 - \frac{2M}{r} + \frac{Q^2}{r^2} \tag{22}$$

and from these equations, one obtains

$$E_{MS} = M - \frac{Q^2}{2r_+} \tag{23}$$

where we have now defined the choice of the horizon as the boundary surface. Had we adopted Einstein's prescription for the pseudo-tensor representing the gravitational field, the same result would be obtained [57]. The energy given by Equation (23) is sometimes defined as "irreducible mass" of the black hole, including the electromagnetic field contribution to the gravitational mass. As a consequence, there is a slight difference between the amount of mass loss and energy loss during the evaporation process. For instance, if the initial charge-to-mass ratio is $y_f = 0.1$, the black hole will lose 90% of its mass and about 95% of its original energy, indicating that about 5% of the electromagnetic energy was lost in the process.

Hence, the black hole "luminosity" was computed here as

$$L = \frac{dE}{dt} = \frac{dE}{dM}\frac{dM}{dt} \tag{24}$$

From Equation (24) and using Equations (12) and (23), one obtains, after some algebra and using the same dimensionless variables,

$$L = -\frac{dy}{dx} + e^x\left[\frac{(y_f/y)^4}{2y^2}\frac{\varepsilon^3}{(1+\varepsilon)^8} + \frac{(y_f/y)^2}{2y^2}\frac{\varepsilon^4}{(1+\varepsilon)^7}\right] \tag{25}$$

Notice that the parameter ε is a function of the initial charge-to-mass ratio and of the mass and should be explicated as in Equation (15).

In the early evolutionary phases, for small charge-to-mass ratios, the horizon temperature, the luminosity, and the charge-to-mass parameter ε do not vary significantly, but near the end, there is a sudden decrease in the parameter ε and a sudden increase in the horizon temperature and luminosity. Almost the totality of the radiated energy occurs in a short time interval, producing in reality a "burst" as it can be seen on the left panel of Figure 3. Increasing the initial charge-to-mass value to $y_f = 0.60$, the behavior of the considered parameters changes dramatically. The parameter ε decreases at a small rate in the very first evolutionary phases, then decreases very rapidly and, in the final phase, goes to zero (extremality) very slowly. Both the temperature and the luminosity increase in the first moments, pass through a maximum (both maxima are close, but they do not coincide exactly), and then decrease and go to zero, as shown on the right panel of Figure 3.

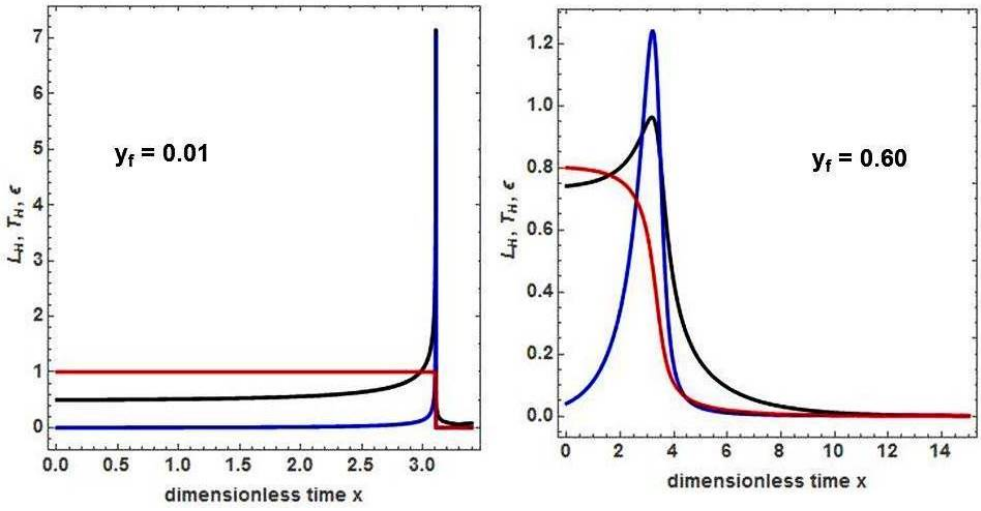

Figure 3. Plot of the luminosity (blue curve), charge-to-mass parameter ε (red curve), and horizon temperature (black curve) as a function of the dimensionless time $x = lg(1 + \tau)$. Ordinates are in arbitrary units in order to permit all curves to be plotted in the same figure. On the left panel, curves correspond to a model characterized by $y_f = 0.01$, while on the right panel, the model is defined by $y_f = 0.60$.

The Horizon Temperature Evolution

The evolution of the horizon temperature as a function of the initial charge-to-mass ratio deserves a more detailed analysis. Extending the thermodynamic concepts of physical systems to black holes, the heat capacity can be defined as

$$C_x = (\partial E/\partial T)_x \tag{26}$$

Notice that some authors [64] define the heat capacity in terms of entropy, that is, $C_x = T(\partial S/\partial T)_x$, but our analysis is not modified by adopting this last definition. In the case of a Schwarzschild black hole, its energy and its horizon temperature depend only on the mass, i.e., $E = M$ and $T = 1/(8\pi M)$ (in natural units). Consequently, one obtains the very well-known result, that is, $C = -8\pi M^2$, or in other words, the heat capacity is negative. This means that, during the evaporation process, the energy of the black hole decreases, but its horizon temperature increases.

The situation is not exactly the same in the case of a RN black hole, since both the energy and the horizon temperature depend now on the mass and on the charge. If the charge is kept constant during the evaporation process, Equation (26) can be rewritten as

$$C_Q = [\partial E(M,Q)/\partial M]_Q / [\partial T(M,Q)/\partial M]_Q \tag{27}$$

For an RN black hole, the energy is given by Equation (23), while the horizon temperature is given as

$$T(M,Q) = \frac{1}{4\pi r_+}\left(1 - \frac{Q^2}{r_+^2}\right) \tag{28}$$

In these equations, we must take into account when computing the derivatives that the horizon radius is also a function of the mass and charge ($r_+ = M(1 + \sqrt{1-(Q/M)^2})$). Computing the heat capacity from Equation (27), using Equations (23) and (28), gives after some algebra

$$C_Q = -\pi M^2 \frac{\left[y_f^2 - 2(1+\sqrt{1-y_f^2})\right]^2}{\left[1 - 2y_f^2 + \sqrt{1-y_f^2}\right]} \tag{29}$$

and as before, y_f is the initial charge-to-mass ratio. It is trivial to show that when $y_f = 0$, the usual Schwarzschild result is recovered. Moreover, Equation (29) has a discontinuity at $y_f = \sqrt{3}/2$, as first remarked in [64]. Therefore, if the initial charge-to-mass ratio is less than $\sqrt{3}/2$, the heat capacity is negative and the horizon temperature increases as the evaporation proceeds. Once the charge-to-mass ratio becomes slightly higher than the critical value, the heat capacity becomes positive and the horizon temperature decreases during the remainder of the evaporation process. Notice that the temperature maximum occurs at the discontinuity point. The discontinuity present in the heat capacity is interpreted by some authors as a "phase transition". However, both the energy and the entropy are continuous at the critical charge-to-mass value, and in this case, the "phase transition" interpretation does not seem to be adequate.

Figure 4 illustrates this behavior, showing the horizon temperature evolution for two initial values of the charge-to-mass ratio y_f. The black curve corresponds to $y_f = 0.40$, a value smaller where the critical value $y_f = \sqrt{3}/2$; the temperature grows initially, passes by a maximum corresponding to the discontinuity point, and then decreases to zero, when the extremality is attained. The blue curve corresponds to $y_f = 0.90$, an initial charge-to-mass ratio higher than the critical value. As expected, the horizon temperature is always decreasing since the heat capacity is positive in this charge-to-mass range.

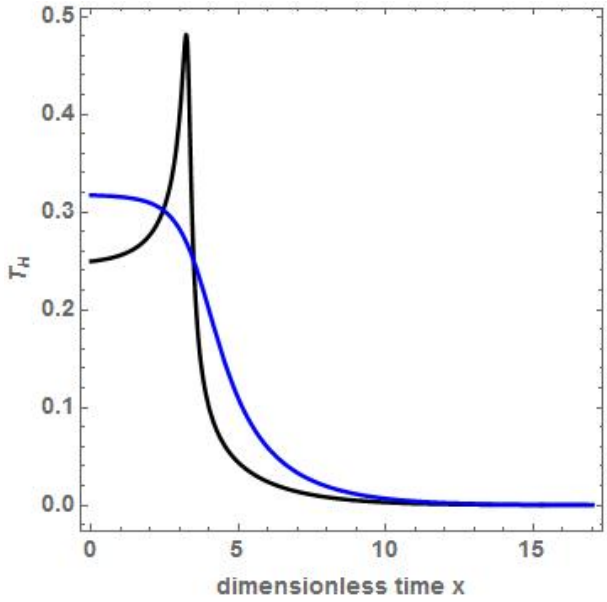

Figure 4. Evolution of the horizon temperature for two different values of the initial charge-to-mass ratio: $y_f = 0.40$ (black curve) and $y_f = 0.90$ (blue curve).

As already mentioned, in our scenario, the initial electric charge present in the collapsing matter is quite small, and as we have seen, the black hole loses a substantial fraction

of its mass before reaching extremality. Moreover, the energy injected by the evaporation process occurs in a very short timescale, as it can be seen on the left panel of Figure 3. It is interesting to check if such a sudden energy injection perturbs the energetics of the cosmic plasma. In Table 1 is given the time interval between the black hole formation at reheating and extremality (column 3) and the cosmic plasma temperature at that moment (column 4). Notice that, taking into account our precedent discussion on coordinate/geodesic time, we have neglected in Table 1 small corrections that are of the order of $\epsilon^{1/3}$.

Table 1. Evaporation timescale and temperature of the cosmic plasma.

T_{rh} (GeV)	M_0/M_P	t_{ev} (s)	T (GeV)
10^{12}	1.48×10^{10}	1.59×10^{-10}	38.0
10^{13}	1.48×10^{8}	1.06×10^{-16}	4.7×10^{4}

The computed timescales given in Table 1 indicate that all the energy injection occurs before nucleosynthesis, which should be expected a priori since the considered PBHs have small masses. However, for the case in which the adopted reheating temperature is 10^{12} GeV, the BHs achieve their evolution around or after the electroweak phase transition, expected to occur at around $T \sim 100$ GeV. In this case, the expected variation of the energy density of the cosmic plasma is

$$\Delta\varepsilon = 1.036 \times 10^{-25} (\Delta E) \left(\frac{M_P}{M_f}\right) f_{BH} \left(\frac{g_{ef}}{g_0}\right) \left(\frac{T}{T_0}\right)^3 \tag{30}$$

where ΔE is the energy lost along the evaporation process, M_f is the BH mass at extremality, f_{BH} is the dark matter fraction in the form of black holes, g_0 and T_0 are respectively the present number of degrees of freedom and the temperature of relativistic matter, and g_{ef} and T are the corresponding values for the considered epoch. For BHs reaching extremality when the temperature of the universe is about 38 GeV, the resulting energy injection corresponds to a ratio of about 2×10^{-8} with respect to the background value. Therefore, these PBHs should not affect the energetic balance of the electroweak phase transition.

These estimates indicate that the evaporation ends quite early and that the nucleosynthesis process should not be affected. However, an investigation in [65] established an upper limit to the charge density present during the nucleosynthesis era in order to avoid perturbations in the helium production process. They derived a charge upper limit of $4.1 \times 10^{-41} \mid e \mid$, where e is the fundamental charge. In our scenario, there is no privileged positive or negative charge excess among PBHs, but statistical fluctuations are expected. In this case, the charge excess density that could be produced by PBHs is

$$n_{ch} = \frac{M}{\mid e \mid} \sqrt{\frac{2Gn_{BH}}{V_H}} \tag{31}$$

where M is the black hole mass when extremality is reached, V_H is the present causal volume of the universe, and n_{BH} is the present BH density that is given by

$$n_{BH} = \frac{3H_0^2 \Omega_{dm}}{8\pi GM} f_{dm} \simeq 1.04 \times 10^{-25} \left(\frac{M_P}{M}\right) f_{dm} \tag{32}$$

where f_{dm} is the fraction of dark matter under the form of PBHs. Using the numbers derived previously, the estimated charge density fluctuation is more than 10 orders of magnitude smaller than the upper bound estimated by [65]. Similarly, using the isotropy of the cosmic microwave background [66], they were able to impose additional constraints on a possible charge asymmetry in the universe. They found that any charge excess per

baryon must be less than $\mid q_+ - q_- \mid < 10^{-26} \mid e \mid$. Using a similar analysis, fluctuations on the charge excess per baryon due to black holes are of the order of

$$\mid q_+ - q_- \mid \simeq \frac{\sqrt{2G}}{\mid e \mid n_b} \left(\frac{n_{BH}}{V_H} \right)^{1/2} M \tag{33}$$

where n_b is the baryon density. The equation above gives for the case $T_{rh} = 10^{12}$ GeV a maximum charge excess of about $2.1 \times 10^{-44} \mid e \mid$, which is about 22 orders of magnitude smaller than the bound imposed by [66].

4. Conclusions

In the present investigation, black holes formed just after the inflaton oscillatory phase, during the reheating, were considered. The masses of these black holes are less than that defined by the causal horizon, since they were scaled by matter fluctuations whose amplitudes are equal or above a critical value derived from numerical simulations of the gravitational collapse. Assuming a Gaussian field for the fluctuations, the initial masses M_0 of these primordial black holes peak at $1.48 \times 10^{10}\ M_P$ and $1.48 \times 10^{8}\ M_P$, corresponding to adopted reheating temperatures, respectively, of $T_{rh} = 10^{12}$ GeV and $T_{rh} = 10^{13}$ GeV.

Despite the absence of a convincing mechanism leading to charge separation in the collapsing matter, we assumed that a small charge could be present due to Poisson fluctuations. As a consequence, a black hole with a small charge-to-mass ratio could be formed at the end of the gravitational collapse. According to our computations, charge-to-mass ratios $Q/\sqrt{G}M_0$ equal to 7.0×10^{-4} and 2.2×10^{-3} result, respectively, if the adopted reheating temperatures are $T_{rh} = 10^{12}$ GeV and $T_{rh} = 10^{13}$ GeV.

Although the initial electric charges in these black holes are rather small, they are able to generate electric fields at the horizon large enough to produce particle–anti-particle pairs, which may discharge the black hole completely. However, as we have discussed previously, some authors claim that the efficiency of the Schwinger mechanism is dramatically weakened when the condition $GM_0m_p/\hbar c = M_0m_p/M_P^2 << 1$ is satisfied. For PBHs having masses of about $10^{10}\ M_p$ and considering massive charged bosons of masses m_p of around 100 GeV, the ratio between the horizon radius and the Compton wavelength of the particle is about 10^{-7}, largely satisfying the latter condition.

Once formed, these PBHs begin to evaporate, and if the initial charge remains constant, they attain the extremal condition and remain stable. The final mass essentially depends on the initial charge-to-mass ratio. Thus, for the parameters mentioned above, the final masses are, respectively, $1.0 \times 10^{7}\ M_P$ and $3.3 \times 10^{5}\ M_P$ if the adopted reheating temperatures are $T_{rh} = 10^{12}$ GeV and $T_{rh} = 10^{13}$ GeV. These are the expected masses if these black holes are considered as possible dark matter candidates.

The evolution of the evaporation process was followed numerically for different initial charge-to-mass ratios y_f. As it can be seen in Figure 2, for $y_f \leq 0.04$, the timescale to reach extremality does not differ appreciably from the evaporation lifetime of a Schwarzschild black hole having the same initial mass. However, for higher values of y_f, the timescale grows almost exponentially. For instance, if $y_f = 0.8$, the timescale to extremality is about 2×10^{6} times the evaporation lifetime of a Schwarzschild black hole of the same mass. These black holes reach extremality well before the nucleosynthesis era and do not perturb the process.

On the one hand, it is well known that the heat capacity of a Schwarzschild black hole is always negative; that is, the horizon temperature increases along the evaporation process. On the other hand, this is not the case in the evolution of a Reissner–Nordstrom black hole since there exists a discontinuity in the heat capacity as the charge-to-mass ratio evolves during the evaporation process. Before the discontinuity, the heat capacity is negative, but beyond this critical point, the heat capacity becomes positive. The critical point corresponds to a charge-to-mass ratio equal to $\sqrt{3}/2 \simeq 0.86602$. Hence, if y_f is initially smaller than the critical charge-to-mass ratio, the horizon temperature increases and then decreases once the

critical point is crossed. Notice that there is no discontinuity in the evolution of the horizon temperature (or in the entropy) at the critical point, which corresponds to the maximum attained horizon temperature. Clearly, if y_f is larger than the critical value, the horizon temperature always decreases along the evaporation process, as illustrated in Figure 4.

In conclusion, charged primordial black holes, after losing a substantial mass fraction by Hawking evaporation, attain extremality, being potential dark matter candidates. Nevertheless, their stability against charge losses depends on future research on the effectiveness of the Schwinger pair production mechanism for very light black holes.

Funding: This research received no external funding.

Data Availability Statement: Data are contained within the article.

Acknowledgments: The author thanks the revisers for their comments, which have improved the presentation of this paper.

Conflicts of Interest: The author declares no conflict of interest.

References

1. Arcadi, G.; Djouadi, A.; Raidal, M. Dark Matter through the Higgs portal. *Phys. Rep.* **2020**, *842*, 1–180. [CrossRef]
2. Chapline, G.F. Cosmological effects of primordial black holes. *Nature* **1975**, *253*, 251–252. [CrossRef]
3. MacGibbon, J.H. Can Planck-mass relics of evaporating black holes close the universe? *Nature* **1987**, *329*, 308–309. [CrossRef]
4. Khlopov, M.Y.; Polnarev, A.G. Primordial black holes as a cosmological test of grand unification. *Phys. Lett. B* **1980**, *97*, 383–387. [CrossRef]
5. Polnarev, A.G.; Khlopov, M.Y. Dustlike stages in the early universe and constraints on the primordial black-Hole spectrum. *Sov. Astron.* **1982**, *26*, 391–395.
6. Khlopov, M.Y.; Malomed, B.A.; Zeldovich, Y.B. Gravitational instability of scalar fields and formation of primordial black holes. *Mon. Not. R. Astron. Soc.* **1985**, *215*, 575–589. [CrossRef]
7. Garcia-Bellido, J.; Linde, A.; Wands, D. Density perturbations and black hole formation in hybrid inflation. *Phys. Rev. D* **1996**, *54*, 6040–6058. [CrossRef]
8. Chen, P. Inflation induced Planck-size black hole remnants as dark matter. *New Astron. Rev.* **2005**, *49*, 233–239. [CrossRef]
9. Cotner, E.; Kusenko, A.; Sasaki, M.; Takhistova, V. Analytic description of primordial black hole formation from scalar field fragmentation. *J. Cosmol. Astropart. Phys.* **2019**, *10*, 077. [CrossRef]
10. Martin, J.; Papanikolaou, T.; Vennin, V. Primordial black holes from preheating instability in single-field inflation. *J. Cosmol. Astropart. Phys.* **2020**, *1*, 024. [CrossRef]
11. Ezquiaga, J.M.; Garcia-Bellido, J.; Morales, E.R. Primordial black hole production in Critical Higgs Inflation. *Phys. Lett. B* **2018**, *776*, 345–349. [CrossRef]
12. Carr, B.; Dimopoulos, K.; Owen, C.; Tenkanen, T. Primordial black hole formation during slow reheating after inflation. *Phys. Rev. D* **2018**, *97*, 123535. [CrossRef]
13. Niemeyer, J.C.; Jedamzik, K. Near-critical gravitational collapse and the initial mass function of primordial black holes. *Phys. Rev. Lett.* **1998**, *80*, 5481–5484. [CrossRef]
14. Bekenstein, J.D. Universal upper bound on the entropy-to-energy ratio for bounded systems. *Phys. Rev. D* **1981**, *23*, 287–298. [CrossRef]
15. de Freitas Pacheco, J.A. Primordial regular black holes: Thermodynamics and dark matter. *Universe* **2020**, *4*, 62. [CrossRef]
16. Page, D.N. Particle emission rates from a black hole: II Massless particles from a rotating hole. *Phys. Rev. D* **1976**, *14*, 3260–3273. [CrossRef]
17. de Freitas Pacheco, J.A.; Silk, J. Primordial rotating black holes. *Phys. Rev. D* **2020**, *101*, 083022. [CrossRef]
18. Chamseddine, A.H.; Mukhanov, V.; Russ, T.B. Black hole remnants. *J. High Energy Phys.* **2019**, *2019*, 104. [CrossRef]
19. Novikov, I.D.; Starobinskii, A.A. Quantum-electrodynamic effects inside a charged black hole and the problem of Cauchy horizons. *Sov. Phys.-JETP* **1980**, *51*, 1.
20. Gibbons, G.W. Vacuum polarization and the spontaneous loss of charge by black holes. *Commun. Math. Phys.* **1975**, *44*, 245–264. [CrossRef]
21. Schwinger, J. On gauge invariance and vacuum polarization. *Phys. Rev.* **1951**, *82*, 664–679. [CrossRef]
22. Kim, S.P.; Page, D.N. Improved approximations for fermion pair production in inhomogeneous electric fields. *Phys. Rev. D* **2007**, *75*, 045013. [CrossRef]
23. Khriplovich, I.B. Radiation of charged particles by a charged black hole. *arXiv* **1999**, arXiv:gr-qc/9812060v1.
24. Page, D.N. Particle emission rates from a black hole. III—Charged leptons from a nonrotating hole. *Phys. Rev. D* **1977**, *16*, 2402–2411. [CrossRef]
25. Gong, Y.; Cao, Z.; Gao, H.; Zhang, B. On neutralization of charged black holes. *Mon. Not. R. Astron. Soc.* **2019**, *488*, 2722–2731.

26. Araya, I.J.; Padilla, N.D.; Rubio, M.E.; Sureda, J.; Magaña, J.; Osorio, L. Dark matter from primordial black holes would hold charge. *J. Cosmol. Astropart. Phys.* **2023**, *2023*, 030.
27. Sorkin, E.; Piran, T. Formation and evaporation of charged black holes. *Phys. Rev. D* **2001**, *63*, 124024.
28. Sorkin, E.; Piran, T. Effects of pair creation on charged gravitational collapse. *Phys. Rev. D* **2001**, *63*, 084006.
29. Sureda, J.; Magana, J.; Araya, I.J.; Padilla, N.D. Press-Schechter primordial black hole mass functions and their observational constraints. *Month. Not. R. Astron. Soc.* **2021**, *507*, 4804–4825.
30. Choptuik, M.W. Universality and scaling in gravitational collapse of a massless scalar field. *Phys. Rev. Lett.* **1993**, *70*, 9–12. [CrossRef]
31. Evans, C.R.; Coleman, J.S. Critical phenomena and self-similarity in the gravitational collapse of radiation fluid. *Phys. Rev. Lett.* **1994**, *72*, 1782–1785. [CrossRef]
32. Koike, T.; Hara, T.; Adachi, S. Critical behavior in gravitational collapse of radiation fluid: A renormalization group (linear perturbation) analysis. *Phys. Rev. Lett.* **1995**, *74*, 5170–5173. [CrossRef]
33. Chongchitnan, S.; Chantavat, T.; Zunder, J. Extreme primordial black holes. *Astron. Notes (Astron. Nachrichten)* **2021**, *342*, 648–657. [CrossRef]
34. Kehagias, A.; Perrone, D.; Riotto, A. Why the universal threshold for primordial black hole formation is universal. *arXiv* **2024**, arXiv:2405.05208.
35. de Freitas Pacheco, J.A.; Kiritsis, E.; Lucca, M.; Silk, J. Quasi-extremal primordial black holes are a viable dark matter candidate. *Phys. Rev. D* **2021**, *107*, 123525. [CrossRef]
36. Ellis, J.; Garcia, M.A.G.; Nanopoulosd, D.V.; Olive, K.A. Calculations of inflaton decays and reheating: With applications to no-scale inflation models. *J. Cosmol. Astropart. Phys.* **2015**, *2015*, 050. [CrossRef]
37. de Freitas Pacheco, J.A. Cosmological stochastic gravitational wave background. In *New Phenomena and New States of Matter in the Universe: From Quarks to Cosmos*; Vasconcellos, C.A.Z., Hess, P.O., Boller, T., Eds.; World Scientific: Singapore, 2023.
38. Kim, S.P.; Lee, H.K.; Yoon, Y. Thermal interpretation of Schwinger effect in near-extremal RN black hole. *Int. J. Mod. Phys. D* **2019**, *28*, 1950139. [CrossRef]
39. Wiscock, W.A.; Weems, L.D. Evolution of charged evaporating black holes. *Phys. Rev. D* **1990**, *41*, 1142–1151. [CrossRef]
40. Jacobson, T. Semiclassical decay of near extremal black holes. *Phys. Rev. D* **1998**, *57*, 4890–4898. [CrossRef]
41. Auffinger, J.; Masina, I.; Orlando, G. Bounds on warm dark matter from Schwarzschild primordial black holes. *Eur. Phys. Plus J.* **2021**, *136*, 261. [CrossRef]
42. Cheek, A.; Heurtier, L.; Perez-Gonzalez, Y.F.; Turner, J. Primordial black hole evaporation and dark matter production: I. Solely Hawking radiation. *Phys. Rev. D* **2022**, *105*, 015022. [CrossRef]
43. Page, D.N. Particle emission rates from a black hole: Massless particles from an uncharged, nonrotating black hole. *Phys. Rev. D.* **1976**, *13*, 198–206. [CrossRef]
44. Calmet, X.; El-Menoufi, B.K. Quantum corrections to Schwarzschild black hole. *Eur. Phys. J. C* **2017**, *77*, 243. [CrossRef]
45. Battista, E. Quantum Schwarzschild geometry in effective field theory models of gravity. *Phys. Rev. D* **2024**, *109*, 026004. [CrossRef]
46. Calmet, X.; Kuipers, F. Quantum gravitational corrections to the entropy of a Schwarzszchild black hole. *Phys. Rev. D* **2021**, *104*, 066012. [CrossRef]
47. Einstein, A.; Strauss, E.G. The influence of the expansion of space on the gravitational fields surrounding the individual stars. *Rev. Mod. Phys.* **1945**, *17*, 120–124. [CrossRef]
48. Israel, W. Discontinuities in spherically symmetric gravitational fields and shells of radiation. *Proc. R. Soc. Lond. A* **1958**, *248*, 404–414.
49. Schucking, E. Das Schwarzschildsche linienelement und die expansion des weltalls. *Z. Phys.* **1954**, *137*, 595–603. [CrossRef]
50. Gautreau, R. Imbedding a Schwarzschild mass into cosmology. *Phys. Rev. D* **1984**, *29*, 198–206. [CrossRef]
51. Sussman, R.A. Conformal structure of a Schwarzschild black hole immersed in a Friedman universe. *Gen. Relativ. Gravit.* **1985**, *17*, 251–291. [CrossRef]
52. Stuckey, W.M. The observable universe inside a black hole. *Am. J. Phys.* **1994**, *62*, 788–795. [CrossRef]
53. Saida, H.; Harada, T.; Maeda, H. Black hole evaporation in an expanding universe. *Class. Quantum Gravity* **2007**, *24*, 4711–4732. [CrossRef]
54. de Freitas Pacheco, J.A. Relativistic accretion into a Reissner-Nordstrom black hole revisited. *J. Thermodyn.* **2012**, *2012*, 791870. [CrossRef]
55. Guarino, D.C.; Horvath, J.E.; de Freitas Pacheco, J.A.; Custodio, P.S. Evolution of primordial black holes in a radiation & phantom energy environment. *Gen. Relativ. Gravit.* **2008**, *40*, 1593–1602.
56. Aguirregabiria, J.M.; Chamorro, A.; Virbhadra, K.S. Energy and angular momentum of charged rotating black holes. *Gen. Relativ. Gravit.* **1996**, *28*, 1393–1400. [CrossRef]
57. Xulu, S.S. Mϕller energy of the nonstatic spherically symmetric metrics. *Astrophys. Space Sci.* **2003**, *283*, 23–32. [CrossRef]
58. Szabados, L.B. Quasi-local energy-momentum and angular momentum in GR: A review article. *Living Rev. Relativ.* **2004**, *7*, 4. [CrossRef]
59. Brown, J.D.; York, J.W. Quasilocal energy and conserved charges derived from the gravitational action. *Phys. Rev. D* **1993**, *47*, 1407–1419. [CrossRef]
60. Hawking, S. Gravitational radiation in an expanding universe. *J. Math. Phys.* **1968**, *9*, 598–604. [CrossRef]

61. Hayward, S. Quasilocal gravitational energy. *Phys. Rev. D* **1994**, *49*, 831–839. [CrossRef] [PubMed]
62. Chen, C.M.; Nester, J.M. Quasilocal quantities for general relativity and other gravity theories. *Class. Quant. Grav.* **1999**, *16*, 1279–1304. [CrossRef]
63. Misner, C.W.; Sharp, D.H. Relativistic equations for adiabatic, spherically symmetric gravitational collapse. *Phys. Rev.* **1964**, *136*, B571–B576. [CrossRef]
64. Davies, P.C.W. The thermodynamic theory of black holes. *Proc. R. Soc. Lond. A* **1977**, *353*, 499–521.
65. Massó, E.; Rota, F. Primordial helium production in a charged universe. *Phys. Lett. B* **2002**, *545*, 221–225. [CrossRef]
66. Caprini, C.; Ferreira, P.G. Constraints on the electrical charge asymmetry of the universe. *J. Cosmol. Astropart. Phys.* **2005**, *2005*, 006. [CrossRef]